RESEARCH ARTICLE

RacA, a Bacterial Protein That Anchors Chromosomes to the Cell Poles

Sigal Ben-Yehuda, David Z. Rudner, Richard Losick*

Eukaryotic chromosomes are anchored to a spindle apparatus during mitosis, but no such structure is known during chromosome segregation in bacteria. When sister chromosomes are segregated during sporulation in *Bacillus subtilis*, the replication origin regions migrate to opposite poles of the cell. If and how origin regions are fastened at the poles has not been determined. Here we describe a developmental protein, RacA, that acts as a bridge between the origin region and the cell poles. We propose that RacA assembles into an adhesive patch at a centromere-like element near the origin, causing chromosomes to stick at the poles.

Sister chromosomes in eukaryotic cells are anchored to the spindle apparatus during mitosis by kinetochores, multiprotein structures that assemble on a specialized region of the chromosome known as the centromere. The spindle apparatus pulls sister chromosomes apart toward opposite poles of the cell via centromere-bound kinetochores (*1*). Sister chromosomes also separate from each other in bacteria in a process that involves the movement of the region of the chromosome containing the origin of replication (bacteria have a single bidirectional origin) toward the cell poles (*2*). Bacteria lack a conspicuous mitotic apparatus, and no equivalent of a kinetochore that anchors the chromosome to a cellular structure is known. Nonetheless, during the cell cycle of *Caulobacter crescentus* and during sporulation in *Bacillus subtilis* newly duplicated origin regions migrate to extreme opposite ends of the cell and appear to be anchored there (*3*).

B. subtilis cells that have begun to sporulate contain two chromosomes that are condensed in an elongated, serpentine-like structure known as the axial filament (*4*). The axial filament extends from pole to pole with the origins located at its ends. A septum then forms near one pole, which divides the developing cell (sporangium) unequally into a forespore (the smaller compartment) and a mother cell (*5*). Formation of the septum traps the origin region of one chromosome in the forespore. Next, a DNA translocase pumps the remainder of the chromosome across the septum into the forespore (*6, 7*). The axial filament was discovered 35 years ago (*4*), but the basis for its formation is mysterious. Also, it is uncertain whether the replication origin regions are truly fastened to the cell poles—and, if so, how. Here we describe a developmental protein named RacA (for remodeling and anchoring of the chromosome) that is required for formation of the axial filament and for anchoring the origin regions at the cell poles.

Remodeling the chromosome. We discovered *racA* (annotated *ywkC*) by building mutants of a large collection of genes whose transcription had been found to be under sporulation control (*8*). Transcription of *racA* was switched on early in sporulation and in a manner that depended on the master regulators for entry into sporulation Spo0A and σ^H (fig. S1A). Immunoblot analysis demonstrated that RacA was present transiently during sporulation (between hours 1.5 and 4 at 30°C; fig. S1B). In keeping with the idea that RacA is dedicated to sporulation, homologs were present in the related spore-forming species *Bacillus anthracis* and *Bacillus halodurans*.

To investigate the role of RacA in sporulation, we treated developing cells with the membrane stain FM4-64 and the DNA stain 4′,6-diamidino-2-phenylindole (DAPI) and visualized them by fluorescence microscopy. We observed three principal effects of the absence of RacA. First, formation of the polar septum was delayed in a RacA mutant; at hour 2 of sporulation, for example, 16% of the wild-type cells but only 4% of the mutant cells had undergone asymmetric division. Second, whereas wild-type cells formed an extended DNA mass (nucleoid) (Fig. 1, A and C), the mutant exhibited a stubby nucleoid (Fig. 1, B and D). Third, wild-type cells trapped DNA in the forespore with high fidelity, but mutant cells that had undergone polar division frequently lacked DNA in the forespore (Fig. 1, B and D). All (350/350) the wild-type sporangia with polar septa examined at hour 2.5 had trapped DNA in the forespore, whereas only 50% (133/268) of the mutant sporangia had done so. Even those mutant sporangia that did succeed in trapping some DNA lacked an axial filament, as indicated by the gap between the nucleoid and the opposite pole of the sporangium (Fig. 1E) and by the relatively small amount of DNA that was trapped in the forespore just after septation (Fig. 1B). Thus, RacA is required for formation of an extended nucleoid and for efficient trapping of DNA in the forespore.

Getting a second chance. The absence of RacA had a severe effect on axial filament formation. Yet, the RacA mutant was only modestly impaired in spore formation (~50% that of the wild type). How are we to explain this apparent contradiction? RacA mutant sporangia that were able to produce DNA-containing forespores sporulated normally. Moreover, many of the mutant sporangia with empty forespores underwent a second round of polar division. Whereas only 4% (11/260) of the wild-type sporangia at hour 3 had undergone septation at both poles, 44% (83/188) of the mutant sporangia exhibited septa near both poles. Of the mutant sporangia with bipolar septa, 61% (76/124) contained DNA in one of the two forespore chambers (see Fig. 1F). Additionally, 36% (45/124) of the bipolar sporangia contained DNA in neither of the forespores (see Fig. 1G).

Sporulating cells have the potential to form septa at both poles but do not do so because the mother cell expresses genes that block cytokinesis at the pole distal to the first-formed septum (*5*). This pathway is triggered by gene expression in the forespore. Mutants blocked in the pathway form aberrant sporangia with septa at both poles (*9*). In RacA mutant sporangia, the absence of DNA in the forespore would interrupt the pathway (by not allowing gene expression in the forespore), thereby allowing cytokinesis to take place at the distal pole of the sporangium. Therefore, the mutant gets a second chance at producing a forespore that has captured DNA. Despite the stubby nature of the nucleoid, the second polar septum frequently succeeds in capturing some chromosomal DNA. The resulting chromosome-containing forespore is able to proceed through the subsequent stages of spore formation despite the presence of an empty forespore at the other end of the sporangium. Sometimes, however, both efforts at trapping DNA fail, resulting in sporangia with empty forespores at both poles. Perhaps even in the wild type the

Department of Molecular and Cellular Biology, Harvard University, 16 Divinity Avenue, Cambridge, MA 02138, USA.

*To whom correspondence should be addressed. E-mail: losick@mcb.harvard.edu

potential to undergo septation at both poles is a fail-safe system that helps to ensure that chromosomal trapping occurs with very high efficiency.

Exclusion of replication origins. As an independent test of the effect of the *racA* mutation on DNA capture by the forespore, we visualized the replication origin region of the chromosome by using green fluorescent protein (GFP) fused to a protein (Spo0J) that binds near the origin (*10*–*12*). Sporangia contain two origins of replication, one for each chromosome. In wild-type sporangia, we observed one fluorescent focus of Spo0J-GFP in the forespore and another at the far end of the mother cell (Fig. 1H). In the case of the RacA mutant, however, both foci were present in the mother cell in about 50% of the cases examined (Fig. 1I). Therefore, RacA is needed for the formation of an elongated nucleoid whose origin regions localize to opposite poles of the cell.

We also examined the localization of the origin proximal-region early after the start of sporulation. In both the wild type and the mutant, we found origin regions to localize at or near opposite poles of these predivisional sporangia (fig. S2). Thus, localization of replication origins occurs in two steps. First, origins move apart to opposite poles in a RacA-independent manner (*13*). Second, the origin regions become anchored at the poles in a process that is mediated by RacA.

RacA localizes to cell poles and the nucleoid. Next, we investigated the localization of RacA itself by using a fusion to GFP. Because RacA fused to GFP was nonfunctional, we used a strain (SB272) harboring *racA* and *racA-gfp*. RacA-GFP was seen as fluorescent foci at the extreme poles of the sporangia, both before and after polar division (Fig. 2A). RacA-GFP also exhibited a haze of fluorescence that colocalized with the nucleoid (Fig. 2A). RacA-GFP was absent, however, from sporangia that had reached the next stage of sporulation in which the forespore is engulfed by the mother cell. Thus,

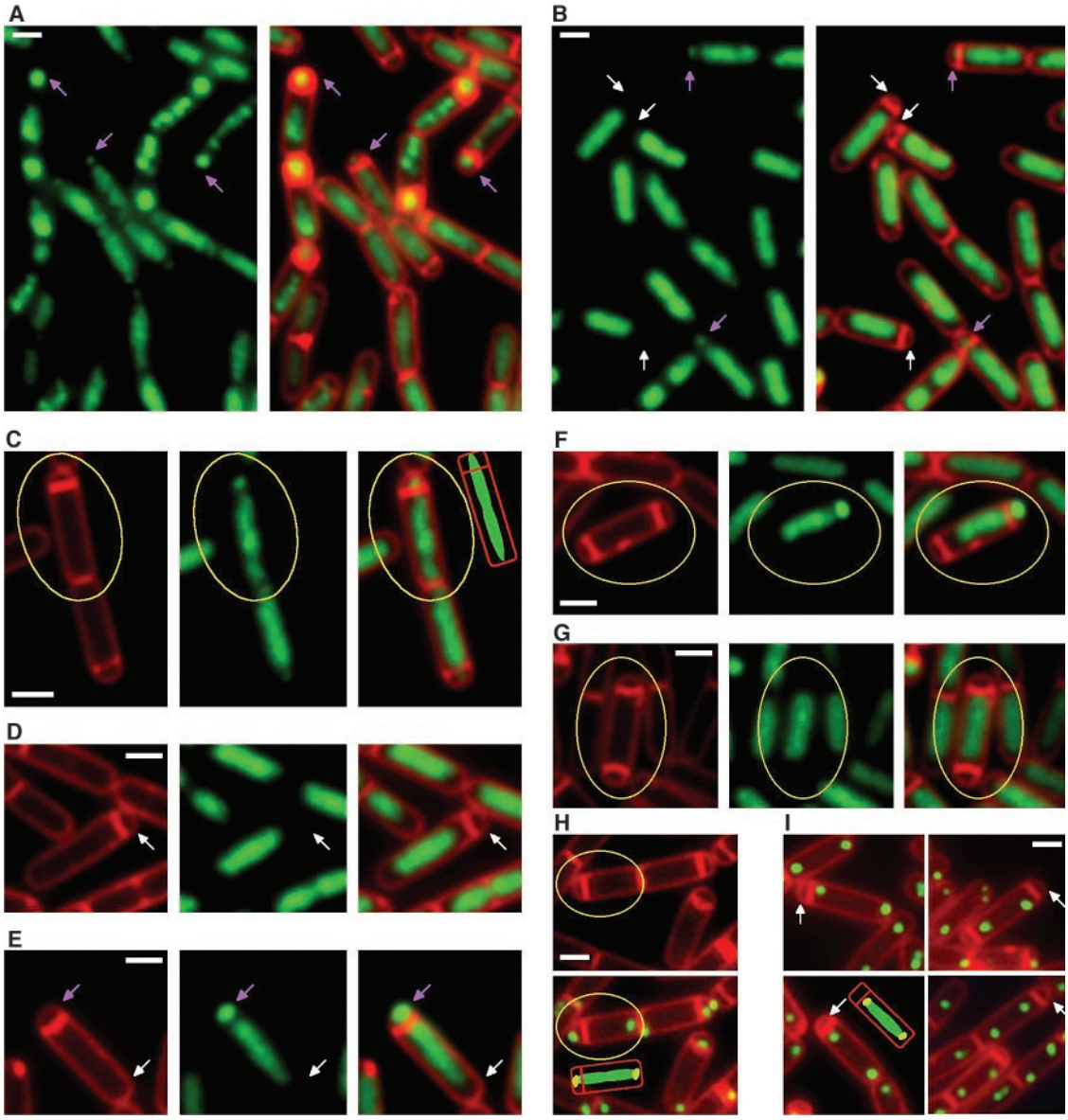

Fig. 1. RacA is required for remodeling and anchoring of the chromosome. Fluorescence microscopy was carried out on cells of strains PY79 (wild type) and SB180 (*racA*Δ::*tet*) at hour 2.5 (**A** to **E**) and hour 3 (**F** and **G**) of sporulation. DNA and membranes were visualized with DAPI (green) and FM4-64 (red), respectively. Wild-type cells (A) and RacA mutant cells (B) show DAPI staining (left panels) and an overlay of FM4-64 and DAPI staining (right panels). Purple arrows point to DNA in the forespore; white arrows point to empty forespores. [(C) to (G)] FM4-64 staining (left), DAPI (center), and overlay (right). (C) Typical axial filament in a wild-type sporangium. Interpretive cartoon shows membrane (red) and DNA (green). (D) RacA mutant sporangium with a typical stubby nucleoid and an empty forespore as indicated by the white arrow. (E) RacA mutant sporangium lacking an axial filament but having trapped DNA in the forespore. Purple arrow points to the forespore; white arrow points to the gap between the forespore-distal edge of the nucleoid and the distal pole. (F) RacA mutant sporangium with bipolar septa that failed to capture DNA in the first polar division but succeeded in the second division. (G) Mutant sporangium with bipolar septa that failed to capture DNA in both polar divisions. (**H**) FM4-64–stained, wild- type sporangium from the Spo0J-GFP–producing strain SB294 at hour 2.5 of sporulation. FM4-64 alone (top) and overlay with Spo0J-GFP (bottom). (**I**) Overlays of four fields of FM4-64–stained, RacA mutant sporangia from the Spo0J-GFP–producing strain SB295 at hour 2.5 of sporulation. White arrows point to the forespore. Interpretive cartoons of sporangia in (H) and (I) show membrane (red), Spo0J-GFP foci (yellow), and DNA (green). Scale bars, 1 μm.

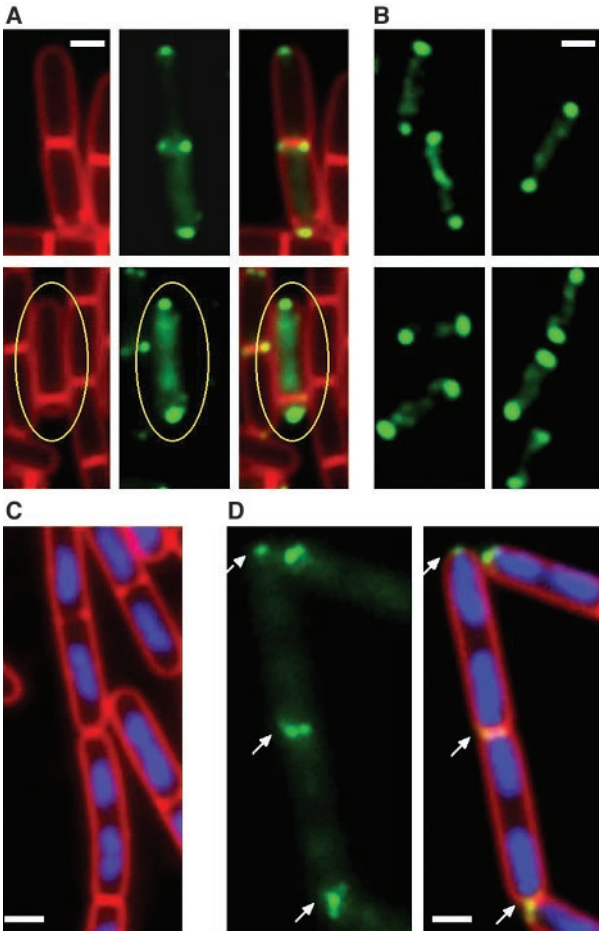

Fig. 2. RacA localizes to the cell poles. (**A**) FM4-64–stained (red) sporangia at hour 2 of sporulation from a RacA-GFP–producing strain (SB272) that harbors *racA* and *racA-gfp*. Upper panels, predivisional sporangia; lower panels, postdivisional sporangium (highlighted by the oval). RacA-GFP (green) is seen as foci at the poles and as a haze over the nucleoids. (**B**) Immunofluorescence staining of sporangia from a wild-type strain (PY79) that had been collected and fixed at hour 2.25 of sporulation and treated with antibodies to RacA. Shown are four fields of stained sporangia. (**C** and **D**) Vegetative cells of a strain (SB281) harboring *racA* and *racA-gfp* under the control of an inducible promoter grown in rich medium with (D) or without (C) the inducer IPTG. Cells were stained with DAPI (blue) and FM4-64 (red). No fluorescence from RacA-GFP was detected in the absence of inducer in (C). (D) Fluorescence (green) from RacA-GFP (left) and an overlay of the RacA-GFP signal with the DAPI and FM4-64 signals (right). Arrows point to polar-localized foci of RacA-GFP. Scale bars, 1 μm.

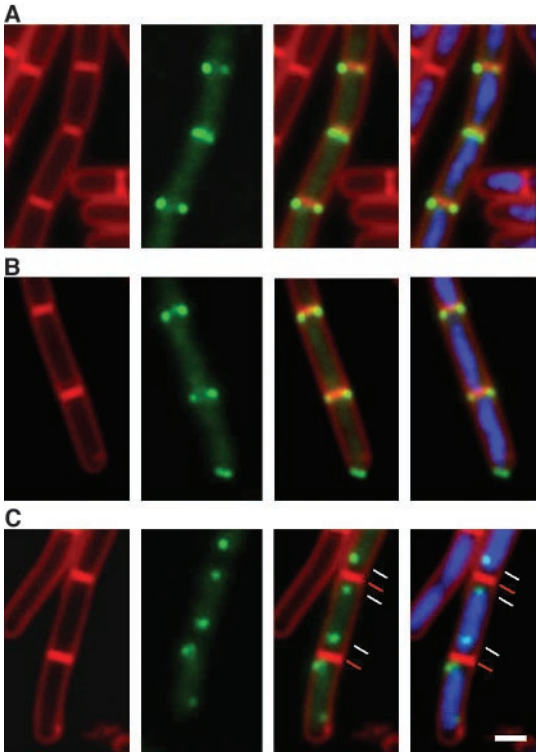

Fig. 3. Localization of RacA to the poles depends on DivIVA. Fluorescence microscopy was carried out at hour 2 of sporulation of cells from a RacA-GFP–producing strain (SB272) (**A**), a RacA-GFP–producing strain that was mutant for MinD (SB314) (**B**), and a RacA-GFP–producing strain that was mutant for MinD and DivIVA (SB319) (**C**). First column shows fluorescence from the membrane stain FM4-64 (red); second column shows fluorescence from RacA-GFP (green); third column shows an overlay of the first two; and fourth column shows an overlay of fluorescence from FM4-64, RacA-GFP, and the DNA stain DAPI (blue). Red lines in (C) point to cell poles; white lines indicate the position of the RacA-GFP foci. Scale bars, 1 μm.

RacA-GFP was present transiently, a finding consistent with the results of immunoblot analysis (fig. S1B).

We also carried out immunofluorescence microscopy with antibodies to RacA. The immunostaining pattern closely resembled that observed with RacA-GFP (Fig. 2B). We observed little or no immunostaining in the RacA mutant control.

These findings suggest that (i) RacA binds throughout the chromosome, helping to remodel the nucleoid into an axial filament; and (ii) it anchors the chromosome to the cell poles. Consistent with the idea that RacA directly binds to DNA, the protein exhibits a putative helix-turn-helix motif in its NH_2-terminal region. (RacA also has two apparent coiled-coil domains.) Moreover, a truncated protein lacking the putative helix-turn-helix localized only to the cell poles. We infer that the NH_2-terminal region is responsible for DNA binding and that the COOH-terminal region is responsible for polar localization.

Anchoring chromosomes. To test whether RacA anchors chromosomes to the poles, we constructed a strain (SB281) in which *racA* and *racA-gfp* were under the control of an isopropyl β-D-thiogalactopyranoside (IPTG)–inducible promoter so that RacA synthesis could be artificially induced during growth. In the absence of IPTG, the cells grew normally, no signal from RacA-GFP was detected, and gaps were present between the nucleoids and the cell poles (Fig. 2C) (fig. S3A). After the addition of inducer, however, foci from RacA-GFP were detected at the poles and in a haze along the nucleoid (Fig. 2D) (fig. S3B). Furthermore, nucleoids in many of the cells (348/400) had shifted to the poles, so that one edge of the nucleoids was closely apposed to a RacA-GFP focus. Thus, RacA localization does not depend on any developmental protein other than RacA itself, and RacA is sufficient to anchor the edge of the nucleoid to the extreme end of the cell.

RacA localization depends on DivIVA. A protein that could be responsible for tethering RacA to the poles is the cell division protein DivIVA. DivIVA is located at the poles, where it sequesters the division inhibitor MinCD, thereby preventing polar division during growth (*14*). Moreover, DivIVA mutants are defective in sporulation and frequently produce empty forespores (*15*). To determine whether polar localization of RacA depends on DivIVA, we investigated the localization of RacA-GFP in a DivIVA mutant. Growth is normally impaired in a DivIVA mutant because, in the absence of the division protein, MinCD is not retained at the cell poles and interferes with medial division (*14*). To circumvent this complication, we used a strain (SB319) that was mutant for MinD as well as for DivIVA (*15, 16*). RacA-GFP localization in a strain (SB314) that was

mutant for MinD alone was largely similar to that observed in the wild type, and axial filament formation seemed to be normal (Fig. 3, A and B). In the MinD DivIVA double mutant, however, RacA-GFP failed to localize to the extreme poles of the sporangium, instead forming foci at the outer edges of the nucleoid (Fig. 3C).

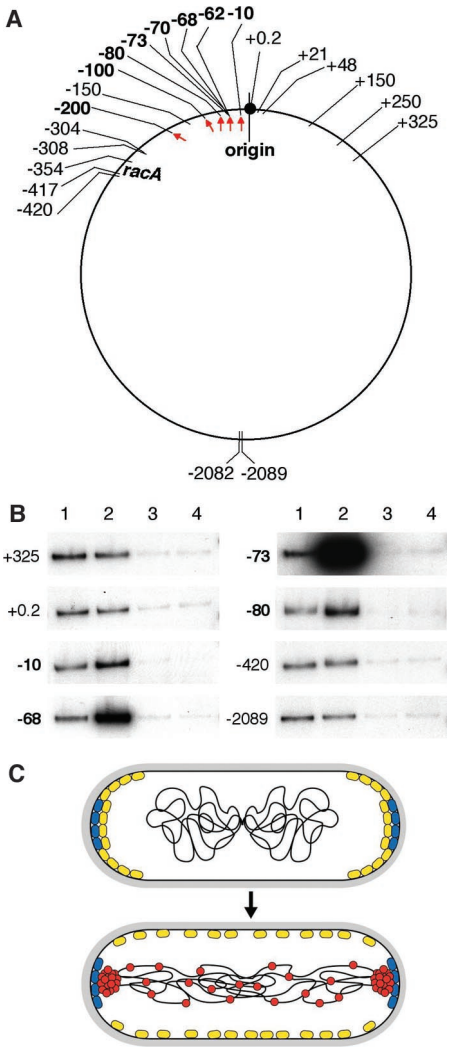

Fig. 4. RacA association with the chromosome. (**A**) Chromosomal sites that were tested for RacA binding by ChIP analysis. Numbers represent the distance from *oriC* in kilobases, with sites to the left of *oriC* indicated with a minus sign and those to the right with a plus sign. Arrows and boldface numbers identify sites of preferential binding by RacA. (**B**) Electropherograms of the products of representative, radiolabeled PCRs for eight of the chromosomal loci (see supporting online material). Lane 1, PCR amplification from total chromosomal DNA; lane 2, amplification from DNA precipitated with antibodies to RacA from an extract of wild-type (PY79) sporulating cells; lane 3, amplification from DNA precipitated with antibodies to RacA from an extract of a RacA mutant (SB180); lane 4, amplification from DNA precipitated with antibodies to GFP from an extract of wild-type (PY79) sporulating cells. Ratios of the signal intensities of lane 2 to lane 1 were 0.7, 0.8, 2.8, 9.1, 21.8, 3.1, 0.9, and 0.8, respectively. (**C**) Model for the role of RacA in chromosomal anchoring and polar division. Top is a vegetative cell; bottom, predivisional sporangium. Symbols represent DivIVA (blue), MinCD (yellow), and RacA (red).

Thus, polar localization of RacA-GFP depends on DivIVA, a finding consistent with the idea that DivIVA is directly or indirectly responsible for sequestering RacA to the cell poles. Also, in addition to its affinity for the nucleoid as a whole, RacA binds with strong preference to a site(s) located near the origin of replication, as inferred from the presence of a bright focus of RacA-GFP near the outer edge of the nucleoid, where the origin is known to be located.

Binding to the chromosome. Chromatin immunoprecipitation (ChIP) experiments were carried out to determine where RacA interacts with the chromosome. We prepared extracts from sporulating cells that had been treated with formaldehyde, which cross-links proteins to DNA. We then used antibodies to RacA to precipitate RacA-DNA complexes from the extracts. Finally, we recovered DNA from the immunoprecipitation and used it as a template for quantitative, radiolabeled polymerase chain reactions (PCRs) with 22 pairs of primers (Fig. 4A). We detected a signal with all the primer pairs, including two from origin-distal locations (Fig. 4B). As controls, little signal was detected with antibodies to GFP or when the ChIP procedure was carried out with sporulating cells from a RacA mutant. These findings are consistent with the cytological experiments, which had indicated that RacA colocalizes with the entire nucleoid. The ChIP experiments also revealed sites of preferential binding close to, and to the left of, the replication origin (Fig. 4, A and B). Once again, the findings are consistent with the cytological experiments, which had revealed a preferential association of RacA-GFP with the origin region of the chromosome. Thus, RacA binds in a dispersed manner throughout the chromosome as well as preferentially to a region of the chromosome located near the origin. Previous work involving large chromosomal rearrangements implicated a region from 214 to 366 kb to the left of the origin in trapping of DNA in the forespore (*17*), but our analysis suggests that preferential binding by RacA is centered 60 to 80 kb from the origin.

Chromosomal anchoring and polar division. We propose the following model for anchoring of chromosomes to the cell poles during sporulation (Fig. 4C). RacA is a kinetochore-like protein that interacts with a centromere-like element located near the replication origin and (directly or indirectly) with the division protein DivIVA, which is sequestered at the cell poles (*14, 15*). We propose that RacA assembles into an adhesive patch that causes the origin region of the chromosome to stick at the pole. Facilitating polar anchoring is the capacity of RacA to bind in a nonspecific manner throughout the entire genome. We suggest that this dispersed mode of binding helps to remodel the nucleoid into an elongated structure, the axial filament, that can reach from pole to pole. Consistent with this remodeling function, RacA is present in high abundance in the sporangium, reaching a concentration (~3000 molecules per cell) similar to that of a protein (SMC) known to cause chromosome condensation in *B. subtilis* (*18*).

RacA may also play a role in polar division. The position of the division septum in bacteria is determined by the site of assembly of the tubulin-like protein FtsZ into a cytokinetic ring (*19, 20*). Formation of the polar septum during sporulation is brought about by a switch in the position of the Z ring from the mid-cell to sites near both poles (although normally cytokinesis occurs at only one polar Z ring) (*21*). This switch is mediated by a spiral intermediate, which could be responsible for redeploying FtsZ molecules from the mid-cell position to the poles, and is caused by an increase in FtsZ levels and by synthesis of an FtsZ-associated protein (*22*). Polar division is normally prevented in growing cells by sequestration of the division inhibitor MinCD, which blocks Z ring formation, to the cell poles (*14, 19, 20*). As noted above, DivIVA is a dual function protein that is responsible for sequestering both MinCD (*14*) and RacA at the poles. We propose that the interactions of MinCD and RacA with DivIVA occur successively and competitively, thereby helping to trigger polar division. In our model (Fig. 4C), RacA displaces MinCD from DivIVA, releasing MinCD from the poles and facilitating polar Z ring formation. Consistent with this proposal, (i) the RacA mutant was delayed in its capacity to form polar septa; (ii) a mutation that blocks the sporulation-specific increase in FtsZ levels, which only mildly impairs polar division on its own, exhibited a synergistic effect when combined with a *racA* mutation; and (iii) induction of high levels of RacA synthesis during growth with an inducible promoter inhibited medial division and caused formation of filamentous cells and the appearance of polar septa, a phenotype that resembles that of a DivIVA mutant (*16, 23*). Thus, RacA could help to link the two principal morphological events that transpire at the onset of development: (i) chromosomal remodeling and anchoring, and (ii) formation of a polar septum. If chromosome-bound RacA causes the release of MinCD from the poles, then the formation of polar Z rings and hence the polar septum would be delayed until the origin regions of the nucleoid reached and became anchored at the cell poles.

References and Notes

1. K. Nasmyth, *Science* **297**, 559 (2002).
2. G. S. Gordon, A. Wright, *Annu. Rev. Microbiol*. **54**, 681 (2000).

3. L. Shapiro, H. H. McAdams, R. Losick, *Science* **298**, 1942 (2002).
4. A. Ryter, P. Schaeffer, H. Ionesco, *Ann. Inst. Pasteur Paris* **110**, 305 (1966).
5. P. J. Piggot, R. Losick, in Bacillus subtilis *and Its Closest Relatives: From Genes to Cells*, A. L. Sonenshein, J. A. Hoch, R. Losick, Eds. (ASM Press, Washington, DC, 2001), pp. 483–517.
6. L. J. Wu, J. Errington, *Science* **264**, 572 (1994).
7. J. Bath, L. J. Wu, J. Errington, J. C. Wang, *Science* **290**, 995 (2000).
8. P. Fawcett, P. Eichenberger, R. Losick, P. Youngman, *Proc. Natl. Acad. Sci. U.S.A.* **97**, 8063 (2000).
9. P. J. Piggot, J. G. Coote, *Bacteriol. Rev.* **40**, 908 (1976).
10. P. Glaser *et al.*, *Genes Dev.* **11**, 1160 (1997).
11. D. C. Lin, P. A. Levin, A. D. Grossman, *Proc. Natl. Acad. Sci. U.S.A.* **94**, 4721 (1997).
12. D. C. Lin, A. D. Grossman, *Cell* **92**, 675 (1998).
13. P. L. Graumann, R. Losick, *J. Bacteriol.* **183**, 4052 (2001).
14. A. L. Marston, H. B. Thomaides, D. H. Edwards, M. E. Sharpe, J. Errington, *Genes Dev.* **12**, 3419 (1998).
15. H. B. Thomaides, M. Freeman, M. El Karoui, J. Errington, *Genes Dev.* **15**, 1662 (2001).
16. D. H. Edwards, J. Errington, *Mol. Microbiol.* **24**, 905 (1997).
17. L. J. Wu, J. Errington, *EMBO J.* **21**, 4001 (2002).
18. J. C. Lindow, M. Kuwano, S. Moriya, A. D. Grossman, *Mol. Microbiol.* **46**, 997 (2002).
19. J. Lutkenhaus, S. G. Addinall, *Annu. Rev. Biochem.* **66**, 93 (1997).
20. W. Margolin, *FEMS Microbiol. Rev.* **24**, 531 (2000).
21. P. A. Levin, R. Losick, *Genes Dev.* **10**, 478 (1996).
22. S. Ben-Yehuda, R. Losick, *Cell* **109**, 257 (2002).
23. J. H. Cha, G. C. Stewart, *J. Bacteriol.* **179**, 1671 (1997).
24. We thank P. Fawcett, A. Rudner, H. Cam, B. Dynlacht, F. Gueiros, and members of the Grossman laboratory (Massachusetts Institute of Technology) for technical advice, strains, and reagents. We thank A. Murray, A. Grossman, J. Errington, L. Shapiro, P. Stragier, and members of R.L.'s laboratory for helpful comments. S.B-Y. is a postdoctoral fellow of the Human Frontier Science Program. Supported by NIH grant GM18568 (R.L.).

Supporting Online Material
www.sciencemag.org/cgi/content/full/1079914/DC1
Materials and Methods
Figs. S1 to S3
Tables S1 and S2
References

29 October 2002; accepted 4 December 2002
Published online 19 December 2002;
10.1126/science.1079914
Include this information when citing this paper.

REPORTS

Deciphering the Reaction Dynamics Underlying Optimal Control Laser Fields

Chantal Daniel,[1] Jürgen Full,[2] Leticia González,[2]* Cosmin Lupulescu,[3] Jörn Manz,[2] Andrea Merli,[3] Štefan Vajda,[3]*† Ludger Wöste[3]

Femtosecond high-resolution pump-probe experiments have been used together with theoretical ab initio quantum calculations and wave packet dynamics simulations to decode an optimal femtosecond pulse that is generated from adaptive learning algorithms. This pulse is designed to maximize the yield of the organometallic ion $CpMn(CO)_5$ while hindering the competing fragmentation. The sequential excitation and ionization of the target ion are accomplished by an optimized field consisting of two dominant subpulses with optimal frequencies and time delays.

With the advent of lasers in the 1960s, great hopes arose for achieving mode selectivity in chemical reactions. However, the rapid internal vibrational redistribution (IVR) makes it difficult to use this approach by trying to excite the bond of interest directly. Ongoing research on femtosecond chemistry (*1*) has since shown that particular reactive pathways can be analyzed and selected by means of well-designed pulses over a range of frequencies (*2*–*6*). For systems with known potential energy surfaces (PESs), several theoretical approaches have demonstrated that laser control can lead to a desired reaction path (*7*–*11*). Some of these strategies have also been verified experimentally in small (typically di- or triatomic) molecules (*1*, *12*, *13*).

In the quest to steer more complex systems, an especially attractive control scheme is adaptive optimal laser pulse control, as introduced by Judson and Rabitz (*14*). An algorithm "teaches" a light field to prepare specific products on the basis of fitness information, such as product yields. This genetic algorithm iteratively creates an optimal laser pulse that prepares the desired target, solving the Schrödinger equation exactly in real time (*14*). This approach was confirmed experimentally first in photophysics by Wilson and co-workers (*15*), and then for manipulating chemical reactions by the group of Gerber (*16*, *17*) and others (*18*–*21*). We have also shown that feedback control can optimize individual fragmentation and ionization paths in $CpMn(CO)_3$ (Cp denotes cyclopentadienyl, η^5-C_5H_5) (*22*). From these applications, the concept of Rabitz and coworkers appears universal, even for finding pathways to products that cannot be prepared easily by means of conventional techniques (*19*).

Nonetheless, the intrinsic information about the dynamics of the system is concealed in the optimal pulses. Detailed analyses that attempt to explain the mechanism of adaptive control have been presented for selective high harmonic generation (*23*) and ionization of atoms (*24*). For complex reactive systems, despite some intuitive working hypotheses (*22*, *25*), the question remains whether the optimal laser field contains a set of rational rules that govern the dynamics. Here, through a combination of femtosecond high-resolution pump-probe experiments and ab initio quantum calculations of the relevant PESs and wave packet simulations, we deciphered the dynamics of a unimolecular reaction induced by an optimal femtosecond pulse, which was generated from adaptive learning algorithms.

We considered laser pulse control of two competing processes in the model system $CpMn(CO)_3$: formation of the parent molecule ion (1a) versus the first "daughter ion" (1b).
In order to understand the mechanism of the experimental optimal laser pulse, we assumed that the control of processes for 1a and 1b exploits different pathways of the laser-induced dynamics; indeed, the deduction of the optimal mechanism requires a comprehensive analysis of these pathways. These processes should involve only a few important degrees of freedom. Here, we focused on the detailed excited state and ion dynamics of the decisive, dissociative metal-ligand bond Mn-CO. An alternative analysis of the preparation of product ions by laser excitation of organometallics, which assumes statistical redistribution of the available energy in all vibrational and rotational degrees of freedom,

[1]Laboratoire de Chimie Quantique, UMR 7551 CNRS/Université Louis Pasteur, Institut Le Bel, 4 Rue Blaise Pascal, 67000 Strasbourg, France. [2]Institut für Chemie-Physikalische und Theoretische Chemie, Freie Universität Berlin, Takustrasse 3, D–14195 Berlin, Germany. [3]Fachbereich Physik, Institut für Experimentalphysik, Freie Universität Berlin, Arnimallee 14, D–14195 Berlin, Germany.

*To whom correspondence should be addressed. E-mail: leti@chemie.fu-berlin.de (L.G.); vajda@physik.fu-berlin.de (S.V.)
†Present address: Argonne National Laboratory, Chemistry Division, 9700 South Cass Avenue, Argonne, IL 60439, USA.